**Atmospheric
Chemistry
and Physics
Discussions**

ACPD

7, 15155–15188, 2007

Nitrogen Oxide
biogenic emissions
from soils

C. Delon et al.

Title Page

Abstract	Introduction
Conclusions	References
Tables	Figures

◄◄   ►►

◄   ►

Back   Close

Full Screen / Esc

Printer-friendly Version

Interactive Discussion

EGU

Nitrogen Oxide biogenic emissions from soils: impact on NO$_x$ and ozone formation in West Africa during AMMA (African Monsoon Multidisciplinary Analysis)

C. Delon[1], C. E. Reeves[2], D. J. Stewart[2], D. Serça[1], R. Dupont[1], C. Mari[1], J.-P. Chaboureau[1], and P. Tulet[3]

[1]Laboratoire d'Aérologie, Université de Toulouse and CNRS, Toulouse, France
[2]School of Environmental Sciences, University of East Anglia, Norwich, UK
[3]CNRM/GMEI, Météo-France, Toulouse, France

Correspondence to: C. Delon (delc@aero.obs-mip.fr)

Abstract

Nitrogen Oxide biogenic emissions from soils are driven by soil and environmental parameters. The relationship between these parameters and NO fluxes is highly non linear. A new algorithm, based on a neural network calculation, is used to reproduce the NO biogenic emissions in West Africa during the AMMA campaign, in August 2006. It has been coupled in the surface scheme of a coupled chemistry dynamics model to estimate the impact of the NO emissions on NO_x and O_3 formation in the lower troposphere. Four different simulations on the same domain and at the same period are compared: CTRL run (without soil NO emissions), YL95 run (with NO emissions inventory, at low time and space resolution), SOILNOx run (with NO emissions from neural network) and ALLNOx run (with NO from neural network). The influence of NO_x from lightning is assessed, and is limited to the upper troposphere. Compared to parameterisations generally used at the global and regional scales, the neural network parameterisation can give higher NO_x (up to +380 ppt) and ozone (up to +7ppb), closer to the ones measured in aircrafts during the AMMA field campaign. The NO emission from soils calculated with neural network responds to changes in soil moisture giving enhanced emissions over the wetted soil, as observed by aircraft measurements after the passing of a convective system, well reproduced by the model. Consecutive enhancement of NO_x and ozone is limited to the lowest layers of the atmosphere in modelling, whereas measurements show higher levels above 500 m. This equation allows an immediate response of fluxes to environmental parameters, on the contrary to fixed emission inventories. The annual cycle of emissions from this algorithm will be simulated in a future work

1 Introduction

NO_x ($NO+NO_2$) react with VOCs (Volatile Organic Compounds) in the presence of sunlight, to form ozone in the troposphere. NO_x concentrations are, among other sources,

directly influenced by NO emitted from soils, which is quickly oxidised to NO_2. Changes in NO sources will consequently modify the rate of ozone production. Estimating biogenic emissions of NO, compared to anthropogenic sources, remains uncertain due to the lack of data. Soil emission processes have been studied in temperate and tropical regions, showing that the main controlling factors are surface soil temperature and moisture, associated with nitrogen deposition and nitrogen content in the soil (Ludwig et al., 2001). Emissions are produced by microbial processes (nitrification/denitrification), and the upscaling of these emissions implies that some simplifications and generalisations are made in the description of the emission processes.

Several modelling approaches have allowed global and regional estimations of NO emissions from soils, leading to various budgets. Potter et al. (1996) proposed a 9.7 TgN/y budget emitted at the global scale, with the CASA (Carnegie-Ames-Stanford) Biosphere model. Yang and Meixner (1997) and Otter et al., (1999) proposed empirical equations based on the response of the emission to surface moisture and temperature at the regional scale. Williams et al. (1992) proposed a regional inventory of biogenic NO emissions in the United States, based on the surface temperature evolution. This algorithm has been improved (taking into account soil moisture and type of biome) and adapted at the global scale by Yienger and Levy (1995), leading to a global budget of 5.5 TgN/yr. Based on this approach, and on field measurements, Yan et al. (2005) have proposed a different algorithm, including different determining parameters (pH, climate, soil organic carbon content, land cover type, nitrogen input), giving a 4.97 TgN/yr budget at the global scale. The majority of current chemistry transport models use the Yienger and Levy inventory for biogenic NO initialisation.

More recently, biogeochemical models have been elaborated, combining the description of nitrification/denitrification processes with climatic evolution of soil parameters (Butterbach-Bahl et al., 2001; Kiese et al., 2005; Kesik et al., 2005), but the application of such models remains only possible in regions where detailed field studies have been conducted. Inverse modelling from satellite mapping (Jaeglé et al., 2004) provides emissions from soils at the global scale, but does not give information on the

relationship between emissions and soil parameters.

Delon et al. (2007) have proposed an original approach for the estimation of NO emissions from soils, based on a neural network calculation. The main advantage of this equation, compared to regional or global existing inventories, is its immediate response to environmental parameters change.

The AMMA (African Monsoon Multidisciplinary Analysis) experiment took place in 2005–2006 and provided a unique dataset over West Africa. AMMA is an international program, with the objective to better understand the African Monsoon mechanisms in terms of dynamics, hydrology, chemistry, and social impacts on local population (Redelsperger et al., 2006; Mari and Prospero, 2005). The Special Observation Periods of the AMMA field campaign took place during the year 2006, in January during the dry season, in June around the monsoon onset and in July and August during the wet season. In particular, several flights and ground based measurements were dedicated to the study of NO_x from soil origin. In this study, we will focus on one particular episode to test the sensitivity of ozone formation to soil NO_x emission. The neural network approach has been implemented on line in a coupled chemistry-dynamics model, MesoNH-Chemistry. The short term impact of NO emissions on ozone budget is studied in the lower troposphere through sensitivity studies and comparison with airborne observations.

2 Model description

2.1 MesoNH-Chemistry

The model used is MesoNH-Chemistry, jointly developed by Meteo-France (Toulouse, France) and the CNRS. A full description of the model is given on http://mesonh.aero.obs-mip.fr/ (Lafore et al., 1998). The horizontal grid consists of 100 by 100 points, with a 20 km resolution. 52 levels are used, from the surface to 30-km height, with 30 levels from 0 to 2000 m. The time step is 30 s. The simulation

EGU

runs from 5 August 2006 00:00 UTC, to 7 August 2006 00:00 UTC. The physics of the model includes a parameterization of deep convection based on mass-flux calculation (Bechtold et al., 2001). This scheme has been adapted by Mari et al. (2006) in order to quantify the amount of lightning NO_x (LiNOx) produced in deep convective clouds. Surface fluxes of energy are provided by the ISBA model (Interactions between Soil Biosphere Atmosphere, Noilhan and Planton, 1989). Biogenic NO emissions from soils, as derived from the neural network approach (Delon et al., 2007) are fully coupled with the model surface scheme (see Sect. 2.2 for details). Anthropogenic emissions and biogenic emission of isoprene and monoterpenes come from the GEIA database (Global Emissions Inventory Activity, www.geiacenter.org).

Large-scale dynamic forcing comes from ECMWF (European Centre for Medium range Weather Forecast) every 6 h, and vertical profiles of background atmosphere are used for chemical initialisation. Initial values for ozone increase from 12 to 40 ppb in the boundary layer, between 0 and 1000 m, and decrease from 2 to 0.05 ppt for NO_x (supposing that no soil source is present). Those values come from standard concentrations that can be found in unpolluted air in West Africa. The chemistry scheme includes 37 chemical species (Crassier et al., 2000; Tulet et al., 2000; Suhre et al., 2000).

2.2 Surface parameters used in the emissions calculation

The calculation of NO emissions with the Atificial Neural Network (ANN) algorithm needs some particular description of soil parameters, such as pH and fertilisation rate, not included in the default version of MesoNH-C. The other parameters (surface moisture, surface and deep soil temperature, and wind speed) are provided by the surface scheme ISBA (or by the atmosphere scheme for the wind speed) at each time step of the simulation. Sand percentage 1b is obtained from the ECOCLIMAP data base (Masson et al., 2003). The pH map is obtained from IGBP-DIS (1998, http://www.sage.wisc.edu/atlas soil database, and is shown in Fig. 1a. The latitudinal variation of pH (low values in the south of the simulation domain) will be a determining

factor for NO emissions. Indeed, Yan et al. (2005) have shown a negative correlation between NO emissions and soil pH in their statistical model, corroborated by Serça et al. (1994).

Quantifying nitrogen fertilization in West Africa is a rather difficult task since mineral
5 fertilizers are poorly used and not documented. The fertilisation rate provided to the model is a constant value in space but not in time, based on organic fertilisation provided by cattle dung. We have estimated the manure input, and assumed assimilation with an exponential decay. This calculation is deduced from Schlecht et al. (1997). Although rough, this estimation has the advantage of providing an estimation of nitro-
10 gen content, as the ANN algorithm needs this information. A detailed map of organic fertilisation based on cattle population would certainly bring an improvement in NO flux estimation. This solution will be investigated in further work.

2.3 Artificial Neural Network algorithm

As mentioned above, an Artificial Neural Network algorithm is used in the surface
15 scheme to provide on line biogenic NO emissions. A full description of the algorithm development can be found in Delon et al. (2007). However, the main information is summarized here.

ANN tools have appeared as alternatives to classical statistical modelling, and are particularly useful for non-linear phenomena. Networks are designed to be able to
20 learn how to represent complex information, and are used to find the best non-linear regression between a number of selected parameters. Namely, an ANN has been used to find the relation between seven parameters or inputs (surface temperature, surface WFPS- Water Filled Pore Space, deep soil temperature (20–30 cm), pH, sand percentage, fertilisation rate, and wind speed) and the output (NO emission fluxes). In order
25 for different situations to be represented, the neural network needs to be supplied with data issued from diverse types of climates and soils. For this purpose, the databases used in this algorithm contain data from temperate and tropical climates. The resulting

EGU

equation is given in Eq. (1):

$$NOflux_{norm} = w_{24} + w_{25}\tanh(S_1) + w_{26}\tanh(S_2) + w_{27}\tanh(S_3) \tag{1}$$

where $NOflux_{norm}$ is the normalized NO flux, and

$$
\begin{aligned}
S_1 &= w_0 + \sum_{i=1}^{7} w_i\, x_{j,norm} \\
S_2 &= w_8 + \sum_{i=9}^{15} w_i\, x_{j,norm} \\
S_3 &= w_{16} + \sum_{i=17}^{23} w_i\, x_{j,norm}
\end{aligned}
\tag{2}
$$
with $j = 1 \rightarrow 7$

where x_1 to x_7 correspond to the seven inputs (surface WFPS, surface soil temperature, deep soil temperature, fertilisation rate, sand percentage, pH and wind speed respectively). pH values used in Delon et al. (2007) have been updated in the tropical part of the database, implying a whole new set of weights (see Table 1).

In the following, in order to test the short term sensitivity of ozone formation to the soil NO_x emission, 4 simulations are discussed, and summed up in Table 2:

– CTRL run: without soil biogenic NO emissions, without LiNOx.

– YL95 run: with biogenic NO emissions from GEIA database (Yienger and Levy, 1995), monthly temporal resolution, 1°/1° spatial resolution, with LiNOx.

– SOILNOX run: with NO emissions from soils calculated on line with the ANN algorithm, including CRF (Canopy Reduction Factor), without LiNOx

– ALLNOX run: with ANN NO emissions from soils and CRF, with LiNOx.

3 Experimental data: NO_x and O_3 concentrations from the UK BAe-146, flight B227

In this study, we will focus on a particular flight during the wet season (flight B227), where chemistry measurements were made. A mesoscale convective system (MCS)

formed over the eastern Niger on 5 August late evening. It reached Niamey on the 6th early morning. On the 6th afternoon, the FAAM (Facility for Airborne Atmospheric Measurements, http://www.faam.ac.uk/) UK BAe-146 Atmospheric Research Aircraft performed a post convective flight (B227) along the MCS track, north east of Niamey

5 (13.5–17.5° N, 2.3–6.5° E, between 13:00 and 17:00 UTC).

Data used in this study concern NO_x and O_3 concentrations. NO_x measurements were made using the University of East Anglia (UEA) NOxy, which measures NO by chemiluminescence and NO_2 by photolytic conversion of NO_2 to NO. Detection limits of the UEA NOxy are ~3 pptv for NO and ~15 pptv for NO_2 with a 10-s integration.

10 Details about this instrument can be found in Brough et al. (2003).

Ozone was measured using a TECO 49 UV photometric instrument. This instrument has been modified with the addition of a drier and separate pressure and temperature sensors. The inlet from the port air sample pipe is pumped via a buffer volume to maintain the inlet air at near surface pressure. All surfaces in contact with the sample

15 including the pump are of Polytetrafluoroethylene (PTFE) or PFA. The instrument has a range of 0–2000 ppbv, a detection limit of 1 ppbv, and a linearity of 2% (as stated by the manufacturer).

4 Simulations comparison and results analysis

The 4 simulations described above are compared in order to understand the respec-

20 tive influence of soil NO_x and LiNOx on ozone formation. The surface emissions are presented first, then the modelling results are described, in terms of NO_x and ozone concentrations, and compared to in situ measurements.

4.1 Comparison between biogenic NO emission maps

The majority of Chemistry Transport Models (CTM) use Yienger and Levy (1995) inven-

25 tory to provide biogenic NO emissions from soils, However, some parts of the world,

like West Africa, are poorly documented, and these emissions lead to an underestimation of concentrations in the lower troposphere (Jaeglé et al., 2005).

Figure 2 shows a comparison between biogenic NO emissions from Yienger and Levy (1995), at monthly and 1°/1° resolution (Fig. 2a), NO emissions calculated from the ANN on 6 August 2006, 15:00 UTC (Fig. 2b), and surface moisture at the same time (Fig. 2c). Emissions from both methods are of the same order of magnitude (1–4 x 10^{10} molec cm^{-2} s^{-1}), with higher mean values for the ANN case. Emissions are more homogeneously distributed in the ANN case, with no null emission occurrence. Furthermore, a Canopy Reduction Factor is applied directly on ANN emissions (detailed further in Sect. 4.2), whereas YL95 emissions are transmitted in their totality to the atmosphere.

The spatial distribution is rather different between the 2 figures, partly due to the difference in spatial resolution of the emissions (1°/1° for YL95, and 20 km/20 km for ANN). The emissions in the ANN case are linked to environmental parameters, and specifically to surface moisture, as shown by the comparison between high emissions in Fig. 2b and strong moisture in Fig. 2c. Indeed, mean surface moisture is stronger in the southern part of the domain where the vegetation is more dense and precipitation events more intense, implying stronger emissions for that part. In the northern part of the domain, emission is more linked to individual precipitation events, inducing intermittently stronger emissions of NO (red circles on Fig. 2b and 2c). When surface moisture decreases in the north, due to the drying of soils after the rain event, emissions decrease as well, whereas they remain stable in the south during the diurnal cycle because of the less fluctuant values of surface moisture. This moisture effect, connected to the latitudinal distribution of pH values, (lower in the south, as shown in Fig. 1a), reinforces the stronger emissions in the south.

Furthermore, strong emissions in the south are also linked to the sand percentage (Fig. 1b): sand ranges from 40 to 90% in the domain, and the strongest emissions are associated with values around 52%. That result has been verified in a field campaign in Hombori (Mali) in July 2004, where the strongest fluxes (30 gN ha^{-1} d^{-1}) were

Title Page

Abstract | Introduction

Conclusions | References

Tables | Figures

◄ | ►I

◄ | ►

Back | Close

Full Screen / Esc

Printer-friendly Version

Interactive Discussion

EGU

EGU

found from a soil where sand percentage was 57% and pH was 6, compared to Sahelian soils with usually 92% sand, and pH around 7, where fluxes ranged between 2–15 gN ha^{-1} d^{-1} (C. Delon, unpublished data).

A rough estimate of global emission in West Africa can be made from this map during the rainy season. If we consider that the emission deduced from the ANN calculation ranges from 0.8×10^{10} to 4.2×10^{10} molec cm^{-2} s^{-1} (which compares well with Ganzeveld et al. (2002) for the same region) a total emission of 0.08–0.6 TgN is calculated for 3 months of the rainy season over West Africa (with an estimated surface of 7800000 km^2). This result may be compared to the annual budget given by Yan et al. (2005) for the entire African continent: 1.373 TgN yr^{-1}.

4.2 Canopy Reduction Factor

A part of the NO emission from soil is deposited onto plants in the form of NO$_2$, this fraction depending on the vegetation density. A simple equation has been implemented in MesoNH-C, considering that CRF is a linear function of LAI (Leaf Area Index), derived from empirical relationships between LAI and NO emission (Yienger and Levy (1995) and references therein, Ganzeveld et al. (2002). Some more complex relations have been developed for specific biomes (Ganzeveld et al., 2002, at the global scale), based on turbulent conditions, diurnal/nocturnal cycle of the boundary layer, and stomatic and cuticular absorption of NO$_2$ onto leaf surface during night and day (Kirkman et al., 2002; Gut et al., 2002). Ultimately, all these equations are closely linked to LAI, and then to NO$_2$ deposition: a large part of the CRF is linked to the NO$_2$ photolysis attenuation below the canopy, and to the efficiency of the NO$_2$ deposition onto leaves. Our choice to simplify these equations leads of course to an approximation of emissions to the atmosphere, but the attenuation is almost 80% efficient in rain forests where the canopy is dense, which is not the case in our domain. In our simulation domain, the LAI does not exceed 3.5 m^2 m^{-2}, leading to a decrease in NO flux reaching 40% at the most. It is important to note here that this study is not focused on CRF parameterisation, hence our choice for a simple parameterisation.

5   Short term impact of soil NO emissions on NO_x and O_3 concentrations in the lower troposphere

Figure 3 shows the comparison between the 4 simulations previously described, at 15:00 UTC between 0 and 2 km height, on a vertical cross section at 2° E, from 21 to 5° N. 15:00 UTC corresponds to the maximum diffusion of surface emitted species due to the maximum development of the boundary layer. Note that the transect between 5 and 21° N covers a large spectrum of vegetation, through mosaic forest, cropland, grassland and desert. YL95 inventory gives a larger magnitude of emissions, compared to the CTRL simulation which is only influenced by anthropogenic emissions (Fig. 3a, YL95-CTRL), a broader distribution of emissions, and a larger impact on NO_x concentrations (difference between the two simulations ranging from 50 ppt to 150 ppt). Figure 3b shows the concentration difference between SOILNOX and CTRL simulations, showing that the introduction of ANN on line emissions coupled with CRF increases the NO_x concentrations in the lower troposphere (up to 450 ppt) stronger than the YL95 simulation does. The impact of ANN emissions (ALLNOX) compared to YL95 emissions, is given in Fig. 3c (ALLNOX-YL95), showing a difference in NO_x concentrations up to 250 ppt.

As NO_x is one of the principal precursors of tropospheric ozone, the impact of NO emissions from soils also has an influence on ozone concentration. Figure 4 shows ozone concentration differences between the 4 simulations. The difference between no emissions and SOILNOX emissions (Fig. 4b) is obvious. The increase of ozone is simulated at all latitudes, showing that even a moderate increase in NO_x concentration leads to dramatic changes in O_3 formation, which is characteristic of NO_x-limited regime. The introduction of on line ANN NO emissions has a significant effect, with a large increase of O_3 concentrations near the surface and at higher altitude (up to 6 ppb between 0 and 2 km). The increase is of the same order of magnitude as with YL95 emissions (Fig. 4a, YL95-CTRL), but with a broader distribution in space. Comparison between YL95 and ALLNOX (Fig. 4c) simulations (LiNOx in both of them) shows a

Nitrogen Oxide biogenic emissions from soils

C. Delon et al.

Title Page

Abstract	Introduction
Conclusions	References
Tables	Figures

⊨◀   ▶⊨

◀   ▶

Back   Close

Full Screen / Esc

Printer-friendly Version

Interactive Discussion

EGU

broader increase of O_3 in ALLNOX (difference up to 4.5 ppb).

LiNOx production occurs where the convection is activated, at altitudes between 8 and 14 km. Lightning accounts for roughly only 15% of the NO_x input to the troposphere (Bradshaw et al., 2000), and is primarily found in the upper troposphere (Pickering et
5 al., 1998) where its lifetime is longer and its ozone producing potential greater (Liu et al., 1987; Pickering et al., 1990) than in the boundary layer. This is verified in our simulations, where the strongest increase in O_3 concentration occurs in the upper troposphere, as shown in Fig. 5. The difference between SOILNOX (without LiNOx) and ALLNOX (with LiNOx) simulations gives the order of magnitude of NOx and ozone pro-
10 duction associated with lightning at the beginning of the night (21:00 UTC), when the effect of convection on chemistry is usually the strongest. NO_x differences range from 0 to 2 ppb around 9–14 km altitude, whereas the maximum O_3 difference is situated around 6–8 km, and may reach 9 ppb.

Once produced inside the convective cloud, NO molecules are redistributed by up-
15 drafts and downdrafts. Ozone is also transported, which could explain why the maximum ozone is not at the same altitude as the maximum NO_x concentration. NO concentrations have been measured up to 12 km height by the DLR Falcon F20 during the AMMA campaign, and range from 0.1 to 1.5 ppb, between 10 and 12 km (H. Schlager, personal communication). Furthermore, Saunois et al. (2007)[1] and Sauvage
20 et al. (2007) state that the average NO_x concentrations in the upper troposphere is ~0.95 ppb, data obtained from the MOZAIC program in West Africa.

---

[1]Saunois, M., Mari, C., Thouret, V., Cammas, J. P., Peyrille, P., Lafore, J. P., Sauvage, B., Volz-Thomas, A., Nedelec, P., and Pinty, J. P.: An idealized two-dimensional model approach to study the impact of the West African monsoon on the tropospheric ozone latitudinal gradient, J. Geophys. Res., in revision, 2007.

EGU

EGU

6   Validation of simulation results with aircraft observations

The comparison between measurements and model is firstly made with the ALLNOX simulation. In order to find which one of the two methods of emission calculation gives the more realistic results in terms of NO_x and O_3 atmospheric concentrations, ALLNOX and YL95 are finally compared.

6.1   Comparison between chemical profiles from model and measurements

As mentioned in paragraph 2.3, ozone and NO_x concentrations were measured in August 2006 onboard the UK BAe aircraft. The B227 flight track is presented in Fig. 6 (6 August). During this flight, the aircraft made a descent profile from 6500 m down to 500 m, between 5.5 and 6.5° E, 16.5 and 17.3° N. O_3 concentrations used in this study were measured during this main profile. After the descent, the aircraft performed a series stack legs around 500 m between 15 and 17° N, 4 and 5° E, and 15:00–16:30 UTC, to sample freshly emitted NO_x air masses. All measured NO_x data below 700 m, between 5 and 18° N, mostly 2–3° E, but extending from 3° W to 6° E, and between 5 to 17 August are also used for comparison with simulated NO_x concentrations on a vertical cut at 4.5° E (6 August 12:00 UTC).

Figure 7 shows the NO_x mixing ratio along the low level run of flight B227. It is worth noting that NO_x mixing ratio decreases from 800 pptv in the south west to 200 pptv in the north east of Niamey. The highest NO_x mixing ratios were observed over an area of moist soil that was wetted by the passing of a convective system on the 5 August (for details see Stewart et al., this issue: Biogenic emissions of NO_x from recently wetted soils over West Africa during the AMMA 2006 campaign). Meso-NH reproduced this convective system, such that an area of enhanced soil moisture is generated in generally the same region (Fig. 2c, red circle crossing the Niger-Mali border). As discussed above, the NO_x emission from soils calculated with ANN responds to changes in soil moisture (Fig. 2b) giving enhanced emissions over the wetted soil within the red circle. These enhanced emissions then lead to elevated concentrations of NO_x (between 200

and 250 ppt) in the lower layers of the model in the location of flight B227 (14–16° N) as illustrated by the cross section along 4.5° E (Fig. 8). This demonstrates that the model is capturing the response of the soil to storm on the 5th August leading to enhanced concentrations of NO_x in the boundary layer as observed during B227.

5   Model results (Fig. 9) show NO_x concentrations ranging mostly between 0 and 400 ppt in the whole simulation domain, (200–300 ppb in the north east of Niamey) at 200 m above ground level (corresponds to 450 m above sea level in the region of Niamey), while measurements during flight B227 (Fig. 7) range from 100 to 800 ppt (mostly between 100 and 400 ppt, average value = 285±152 ppt) between 15 and
10 17° N. Roughly, the range of measured concentrations is reproduced by the model.

     NO_x data measured below 700 m during all the flights in August 2006 are illustrated in Fig. 10 and provide a synthetic regional view of NO_x latitudinal distribution. NO_x data range from 100 to 800 ppt between 5 and 18° N, with means for 0.5 latitude bins mostly being below 400 ppt. Note that the higher concentrations around 7° N are from
15 anthropogenic sources around Lagos. The concentrations around 400–800 ppt north of 14° N are mostly related to recently wetted soils (Stewart et al., this issue).

     Below 500 m, the model gives values in the range of measured data (Fig. 8). With the exception of Lagos (7° N), and north of the vegetated areas, there is a slight increasing gradient of NO_x from south to north in measurements (Fig. 10) which is not found in the
20 model (Fig. 8). This could be due to several reasons: the pH effect on NO emissions is overestimated in the south of the domain, and CRF effect is not strong enough, due to an underestimation of vegetation cover. Further work is planned on these two topics to improve the spatial repartition of NO fluxes.

     Above 500 m, and at the top of the boundary layer, model concentrations are repre-
25 sentative of background concentrations and are far lower than measured values (25 ppt in the model (Fig. 8) versus 200 ppt at 2000 m from the aircraft, not shown here). The enhanced mixing ratios simulated only below 500 m can be attributed to the inefficient response of the turbulent scheme to the enhanced soil humidity. Furthermore, a tongue of low NO_x coming down around 14–17° N seems to be driven by a strong descent of

EGU

air from above. The underestimation above 500 m may be explained by the dynamics: slow vertical diffusion leads to the highest concentrations being in the boundary layer near the surface, with low concentrations (<25 ppt) higher in the boundary layer. The dynamical structure of the lower layers of the atmosphere is different in the model and

5   from that observed. A mixed layer is retrieved in the data from surface up to 4000 m (as stated by the B227 mission report), whereas the model shows a strong stratification between the boundary layer and the layer above. These differences in dynamical structures involve differences in the transport and mixing and processing of chemical species emitted at the surface. Further insight in the dynamical behaviour of the bound-

10 ary layer for this particular episode is needed to improve the understanding of chemical vertical distribution.

Measured ozone concentrations range from 26 ppb in the south of the domain to 40 ppb in the north east of Niamey at 500 m height above sea level. This latitudinal gradient is correctly reproduced in the model (not shown here), with correct orders of

15 magnitude (20 to 45 ppb from south to north). However, simulated O_3 mixing ratios are slightly underestimated (34–35 ppb) in the north east of Niamey where the BAe 146 flew. These differences are consecutive to the differences in dynamical structures between model and measurements, as explained above.

Figure 11 gives a more precise idea of the difference of impacts between YL95

20 and ALLNOX simulations, over the whole domain, at 200 m height above ground level (~450 m above sea level in the Niamey region). Differences in NO_x concentrations at this altitude reaches 370 ppt (ALLNOX>YL95, Fig. 11a), and ozone difference ranges between −2 and +7 ppb, with most being positive values (positive difference means that ALLNOX>YL95, Fig. 11b). As a consequence, the ALLNOX simulation gives

25 higher levels of ozone and NO_x than the YL95 simulation. The ANN model is an improvement on YL95, but there is still further work that can be done.

7 Summary and conclusion

The influence of soil biogenic NO emissions on ozone and NO_x concentrations over West Africa is assessed in the framework of the AMMA campaign. A specific algorithm of emission has been processed by a neural network, and has been inserted on-line into the model MesoNH-Chemistry. It is compared to the Yienger and Levy inventory (monthly and 1°/1° resolution) through the influence on NO_x and O_3 atmospheric concentrations. ANN emissions are differently distributed in space (with stronger emissions in the south of the simulation domain), and follow the evolution of environmental parameters, specifically surface moisture, at the time step of the model.

The results of 4 different 48h simulations in a 2000 km/2000 km domain in West Africa, centred near Niamey, Niger, are compared to assess the impact of these ANN emissions. NO_x emissions from lightning are introduced in 2 simulations, the first with Yienger and Levy (1995) emissions, the second one with ANN emissions. The influence of LiNOx is obvious around 10 km altitude, and can also be slightly identified in the boundary layer. The influence of ANN emissions on NO_x and ozone concentration is stronger than YL95 emissions, and in places involves an increase of 2 to 8 ppb of ozone in the lower troposphere (0–2000 m). The main advantage of the ANN algorithm is its immediate connection to surface temperature and moisture, key parameters in tropical climate for biogenic NO emissions. Fixed inventories do not allow this immediate response of emissions.

These modelling results have been compared to measurements performed during the AMMA campaign between 5 and 17 August for NO_x. ANN leads to enhanced fluxes over the wetted soils, as observed by the aircraft, and to enhanced NO_x concentrations close to the surface (up to 200 m above ground level), in the range of measured data. A pretty good agreement has been found between modelled and measured concentrations on the 6 August, where the model reproduces correctly the passing of a convective system and the observed resulting NO_x enhancement. However, the spatial distribution of modelled NO_x concentrations does not exactly correspond to the

15170

measured one: further insight in pH impact on NO emissions, and a correct estimate of vegetation cover in the south of the domain would certainly improve the spatial features of NO fluxes. The increase of NO_x concentrations leads to an immediate increase in ozone concentrations in the model, which is characteristic of NO_x-limited regimes. The vertical diffusion of NO_x is limited to the lowest layers of the atmosphere, but the correct estimate of NO emissions (in terms of magnitude) leads to an improvement of NO_x and O_3 levels near the surface. Uncertainties remain in relation with environmental parameters, but this equation helps to improve the quantification of biogenic NO emissions in a region where seldom data are available. This algorithm will be used in the future in surface modelling to test its validity during all seasons of West Africa (annual cycle of emissions) at the continental scale.

References

Baker B., Bai, J. H., Johnson, C., Cai, Z. T., Li, Q. J., Wang, Y. F., Guenther, A., Greenberg, J., Klinger, L., Geron, C., and Rasmussen, R.: Wet and dry season ecosystem level fluxes of isoprene and monoterpenes from a southeast Asian secondary forest and rubber tree plantation, Atmos. Env. 39, 381–390, 2005.

Bechtold, P., Bazile, E. Guichard, F. Mascart, P., and Richard, E.: A mass flux convection scheme for regional and global models, Q. J. R. Meteorol. Soc., 127(573), 869–886, 2001. 15159

Bradshaw, J., Davis, D., Grodzinsky, G., Smyth, S., Newell, R., Sandholm, S., and Liu, S.:

Observed distributions of nitrogen oxides in the remote free troposphere from the NASA global tropospheric experiment programs, Rev. Geophys., 38(1), 61–116, 2000. 15166

Brough, N., Reeves, C. E., Penkett, S. A. Stewart, D. J., Dewey, K., Kent, J., Barjat, H., Monks, P. S., Ziereis, H., Stock, P., Huntrieser, H., and Schlager, H.: Intercomparison of aircraft instruments on board the C-130 and Falcon 20 over southern Germany during EXPORT 2000, Atmos. Chem. Phys., 3, 1–12, 2003, http://www.atmos-chem-phys.net/3/1/2003/. 15162

Butterbach-Bahl, K, Stange, F., Papen, H., and Li, C: Regional inventory of nitric oxide and nitrous axide emissions for forest soils of southeast Germany using the biogeochemical model PnET-N-DNDC, J. Geophys. Res., 106, 34 155–34 166, 2001. 15157

Crassier, V., Suhre, K., Tulet, P., and Rosset, R.: Development of a reduced chemical scheme for use in mesoscale meteorological models, Atmos. Env., 34(16), 2633–2644, 2000. 15159

Delon C., Serça, D., Boissard, C., Dupont, R., Dutot, A., Laville, P., de Rosnay, P., and Delmas, R.: Soil NO emissions modelling using artificial neural network, Tellus B, 59B, 502–513, 2007. 15158, 15159, 15160, 15161, 15177

Ganzeveld, L. N., Lelieveld, J., Dentener, F. J., Krol, M. C., Bouwman, A. J., and Roelofs, G. J.: Global soil-biogenic NOx emissions and the role of canopy processes, J. Geophys. Res., 107(D16), 10.1029/2001JD001289, 2002. 15164

Gut, A., Scheibe, M., Rottenberger, S., Rummel, U., Welling, M., Ammann, C., Kirkman, G. A., Kuhn, U., Meixner, F. X., Kesselmeier, J., Lehmann, B. E. Scmidt, W. Müller, E., and Piedade, M. T. F.: Exchange fluxes of NO_2 and O_3 at soil and leaf surfaces in an Amazonian rain forest, J. Geophys. Res., Vol. 107, D20, 8060, doi:10.1029/2001JD000654, 2002. 15164

Jaeglé, L., Martin, R. V., Chance, K., Steinberger, L., Kurosu, T. P., Jacob, D. J., Modi, A. I., Yoboué, V., Sigha-Nkamdjou, L., and Galy-Lacaux, C., 2004: Satellite mapping of rain-induced nitric oxide emissions from soils, J. Geophys. Res., 109, doi:10.1029/2003JD004406, 2004. 15157

Jaeglé, L., L. Steinberger, V., Randall, M., and Chance, K.: Global Partitioning of NOx sources using satellite observations: Relative role of fossil fuel combustion, biomass burning and soil emissions, Faraday Discuss., 130, 407–423, 2005. 15163

Kesik, M., Ambus, P., Baritz, R., Brüggemann, N., Butterbach-Bahl, K., Damm, M., Duyser, J., Horvath, L., Kiese, R., Kitzler, B., Leip, A., Li, C., Pihlatie, M., Pilegaard, K., Seufert, G., Simpson, D., Skiba, U., Smiatek, G., Vesala, T., and Zechmeister-Boltenstern, S.: Inventories of N2O and NO emissions from European forest soils, Biogeosciences, 2, 353–375, 2005, http://www.biogeosciences.net/2/353/2005/. 15157

Title Page

Abstract | Introduction

Conclusions | References

Tables | Figures

◄ | ►

◄ | ►

Back | Close

Full Screen / Esc

Printer-friendly Version

Interactive Discussion

EGU

Kiese, R., Li, C., Hilbert, D. W., Papen, H., and Butterbach-Bahl, K.: Regional application of PnET-N-DNDC for estimating the N2O source strength of tropical rainforests in Wet Tropics of Australia, Global Change Biol., 11(1), 128–144, 2005. 15157

Kirkman, G. A., Gut, A., Ammann, C., Gatti, L. V., Cordova, A. M., Moura, M. A. L., Andreae, M. O., and Meixner, F. X.: Surface exchange of nitric oxide, nitrogen dioxide, and ozone at a cattle pasture in Rondonia, Brazil, J. Geophys. Res., 107, D20, 8083, doi:10.1029/2001JD000523, 2002. 15164

Lafore, J.-P., Stein, J., Asencio, N., Bougeault, P., Ducrocq, V., Duron, J., Fischer, C., Hereil, P., Mascart, P., Pinty, J.-P., Redelsperger, J.-L., Richard, E., and Vila-Guerau de Arellano, J.: The Meso-NH Atmospheric simulation system, I. Adiabatic formulation and control simulations, Ann. Geophys., 16, 90–109, 1998, http://www.ann-geophys.net/16/90/1998/. 15158

Liu, S. C., Trainer, M., Fehsenfeld, F. C., Parrish, D. D., Williams, E. J., Fahey, D. W., Hubler, G., and Murphy, P. C.: Ozone production in the rural troposphere and the implications for regional and global ozone distributions, J. Geophys. Res., 92, 4191–4207, 1987. 15166

Ludwig, J., Meixner, F. X., Vogel, B., and Frstner, J.: Soil-air exchange fo nitric oxide: An overview of processes, environmental factors, and modelling studies, Biogeochemistry, 52, 225–257, 2001. 15157

Mari, C. and Prospero, J.: African Monsoon Multidisciplinary Analysis-Atmospheric Chemistry (AMMA-AC): a new IGAC task; IGACtivities Newsletter, 31, 2–13, 2005. 15158

Mari, C., Chaboureau, J.-P., Pinty, J.-P., Duron, J., Mascart, P., Cammas, J.-P., Gheusi, F., Fehr, T., Schlager, H., Roiger, A., Lichtenstein, M., and Stock, P.: Regional lightning NO_x sources during the TROCCINOX experiment, Atmos. Chem. Phys., 6, 3487–3503, 2006, http://www.atmos-chem-phys.net/6/3487/2006/. 15159, 15177

Masson, V., Champeaux, J.-L., Chauvin, F., Meriguet, C., and Lacaze, R.: A global database of land surface parameters at 1-km resolution in meteorological and climate models, J. Climate, 16(9), 1261–1282, 2003. 15159

Meyer-Arnek, J., Ladstätter-Weissenmayer, A., Richter, A., Wittrock, F., and Burrows, J.: A study of the trace gas columns of O_3, NO_2 and HCHO over Africa in September 1997, Faraday Discuss., 130, 387–405, doi: 10.1039/b502106p, 2005.

Noilhan, J. and Planton, S.: A simple parameterization of land surface processes for meteorological models, Mon. Wea. Rev., 117, 536–549, 1989. 15159

Otter, L. B., Yang, W. X., Scholes, M. C., and Meixner, F. X.: Nitric oxide emissions from a Southern African Savanna, J. Geophys. Res., 104, 18 471–18 485, 1999. 15157

Title Page

Abstract | Introduction

Conclusions | References

Tables | Figures

|◄ | ►|

◄ | ►

Back | Close

Full Screen / Esc

Printer-friendly Version

Interactive Discussion

EGU

Pickering, K. E., Thompson, A. M., Dickerson, R. R., Luke, W. T., McNamara, D. P., Greenberg, J., and Zimmermann, P. R.: Model calculations of tropospheric ozone production potential following observed convective events, J. Geophys. Res., 95, 14 049–14 062, 1990. 15166

Pickering, K. E., Wang, Y., Tao, W. K., Price, C., and Müller, J. F.: Vertical distributions of lightning NO_x for use in regional and global chemical transport models, J. Geophys. Res., 103, 31 203–31 216., 1998. 15166

Potter, C. S., Matson, P. A., Vitousek, P. M., and Davidson, E. A.: Process modelling of controls on nitrogen trace gas emissions from soils worldwide, J. Geophys. Res., 101, 1361–1377, 1996. 15157

Redelsperger, J.-L., Thorncroft, C. D., Diedhiou, A., Lebel, T., Parker, D. J., and Polcher, J.: African Monsoon Multidisciplinary Analysis: An International Research Project and Field Campaign, Bull. Amer. Meteor. Soc., 87, 1739–1746, 2006. 15158

Sauvage, B., Thouret, V., Cammas, J.-P., Brioude, J., Nedelec, P., and Mari, C.: Meridional ozone gradients in the African upper troposphere, Geophys. Res. Lett., 34 (3), 03817, 2007. 15166

Schlecht, E., Fernandez-Rivera, S., and Hiernaux, P.: Timing, size and nitrogen concentration of faecal and urinary excretions in cattle, sheep and goats: Can they be exploited for better manuring of cropland?, in: Soil Fertility Management in West African Land Use Systems, edited by: G. Renard, A. Neef, K. Becker and M. von Oppen, Niamey, Niger, Margarf Verlag, Weikersheim, Germany, 1997. 15160

Serça, D., Delmas, R., Jambert, C., and Labroue, L.: Emissions of nitrogen oxides from equatorial rain forest in central Africa: origin and regulation of NO emissions from soils, Tellus 46B, 243–254, 1994. 15160

Suhre, K., Crassier, V., Mari, C., Rosset, R., Johnson, D. W., Osborne, S., Wood, R., Andreae, M. O., Bandy, B., Bates, T. S., Businger, S., Gerbig, C., Raes, F., and Rudolph, J.: Chemistry and aerosols in the marine boundary layer: 1-D modelling of the three ACE-2 Lagrangian experiments, Atmos. Env., 34, 5079–5094, 2000. 15159

Tulet, P., Crassier, V., and Rosset, R.: Air pollution modelling at a regional scale, Environmental Modelling and Software, 15 693–15 701, 2000. 15159

Williams, E. J., Guenther, A., and Fehsenfeld, F. C.: An inventory of nitric oxide emissions from soils in the United States, J. Geophys. Res., 97, 7511–7519, 1992. 15157

Yan, X., Ohara, T., and Akimoto, H.: Statistical modelling of global soil NO_x emissions, Global Biogeochem. Cycles, 19, GB3019, doi:10.1029/2004GB002276, 2005. 15157, 15160, 15164

Nitrogen Oxide biogenic emissions from soils

C. Delon et al.

Title Page

Abstract	Introduction
Conclusions	References
Tables	Figures

◀◀   ▶▶

◀   ▶

Back   Close

Full Screen / Esc

Printer-friendly Version

Interactive Discussion

EGU

Yang, W. X. and Meixner, F. X.: Laboratory studies on the release of nitric oxide from subtropical grassland soils: The effect of soil temperature and moisture, in: Gaseous Nitrogen Emissions from Grasslands, edited by: S. C. Jarvis, B. F. Pain, pp. 67–70, CAB International, Wallingford, New York, 1997. 15157

5 Yienger, J. J. and Levy, H. II: Empirical model of global soil-biogenic NO_x emissions, J. Geophys. Res., 100, 11 447–11 464. 1995 15157, 15161, 15162, 15163, 15164, 15170, 15177, 15179

Nitrogen Oxide biogenic emissions from soils

C. Delon et al.

Title Page

Abstract	Introduction
Conclusions	References
Tables	Figures

|◄ ►|

◄ ►

Back	Close

Full Screen / Esc

Printer-friendly Version

Interactive Discussion

EGU

EGU

Table 1. Weights for NO flux modelling with neural network parameterization, to be used in Eq. (1).

w0	0.561651794427011	w14	1.61126351888328
w1	−0.48932473825312	w15	0.134088164903734
w2	−0.33521035872982	w16	−0.21261983875851
w3	0.506600069632212	w17	0.901773966331639
w4	−0.784867014304196	w18	−1.18779902340853
w5	0.283241716518431	w19	1.23132977162784
w6	0.132539461337082	w20	−2.62451302093078
w7	−0.008396615495977	w21	−0.27778477919531
w8	−1.62075908632141	w22	0.413060247967231
w9	0.638173941854311	w23	−0.56046255255612
w10	3.88469485689393	w24	0.499562769416134
w11	−0.942985468044301	w25	−1.23876483956298
w12	−0.862455616914003	w26	−1.41295235373665
w13	−2.68040193699105	w27	−1.20659105237301

Table 2. Simulation configurations.

Run name	CTRL	YL95	SOILNOX	ALLNOX
Biogenic NO emissions	No	Yienger and Levy (1995)	Delon et al. (2007)	Delon et al. (2007)
Canopy Reduction Factor	No	No	Yes	Yes
Lightning NO$_x$ (LiNOx)	No	Mari et al. (2006)	No	Mari et al. (2006)

Full Screen / Esc

Printer-friendly Version

Interactive Discussion

EGU
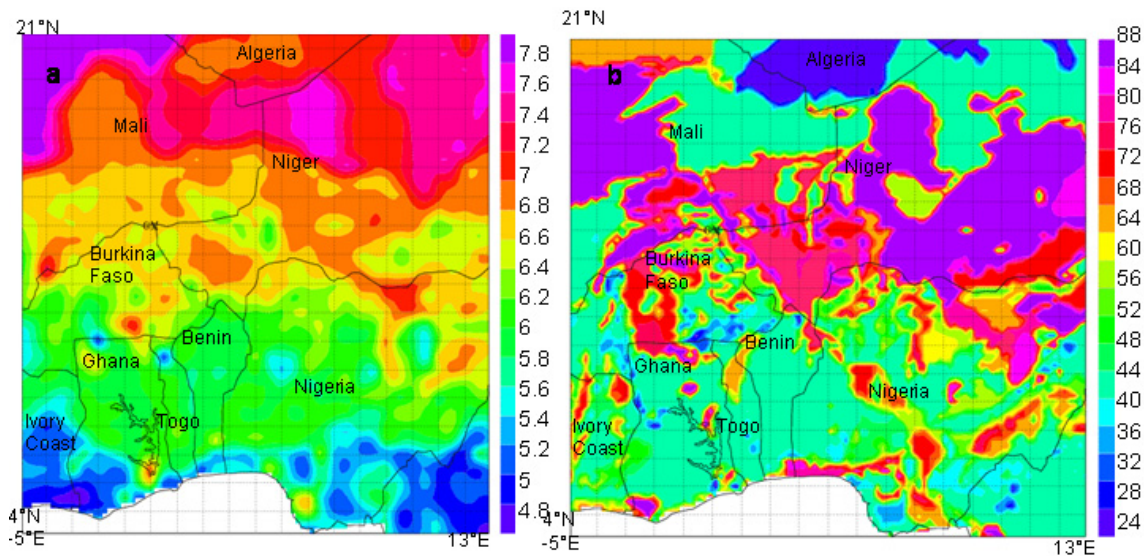
Fig. 1. (a) pH values and **(b)** sand percentage in the simulation domain.
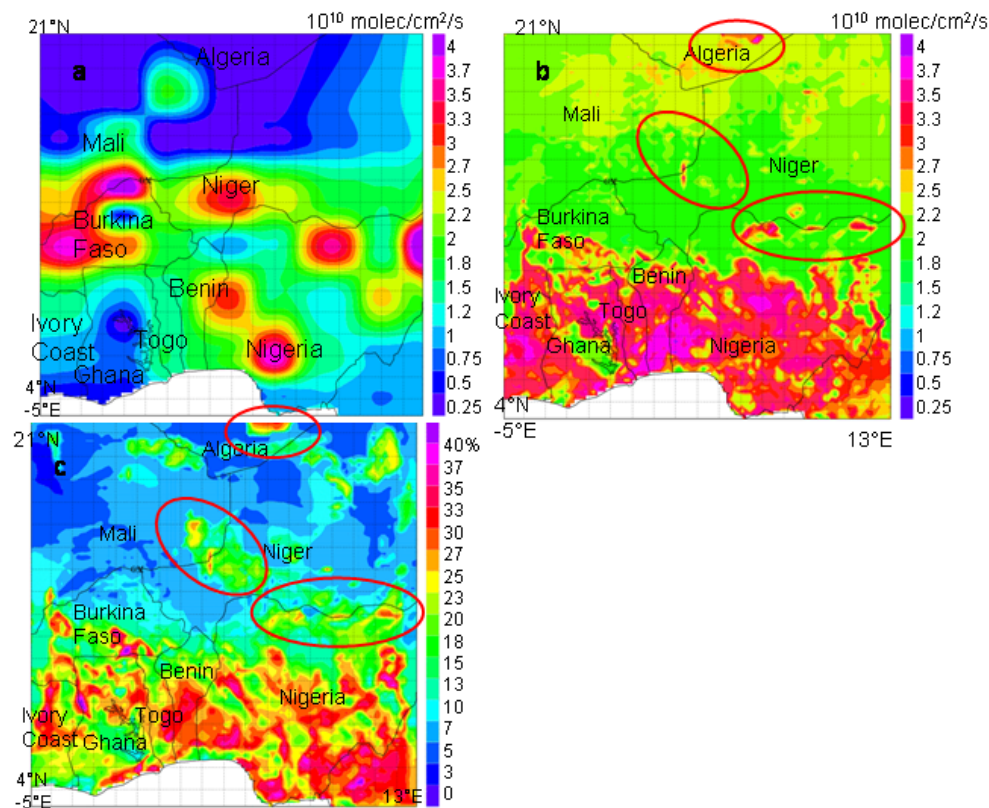
Fig. 2. **(a)** Biogenic NO emissions from soil (1010 molec.cm^{-2}.s^{-1}) in August, provided by GEIA database, from Yienger and Levy (1995) inventory, **(b)** biogenic emissions from soils (10^{10} molec cm^{-2} s^{-1}) provided by the on line ANN algorithm, 6 August 2006 15:00 UTC, and **(c)** soil moisture (%), 6 August 2006 15:00 UTC. Red circles highlight the correspondence between strong moisture and high emissions.

Title Page

Abstract | Introduction

Conclusions | References

Tables | Figures

|◀ | ▶|

◀ | ▶

Back | Close

Full Screen / Esc

Printer-friendly Version

Interactive Discussion

EGU

EGU
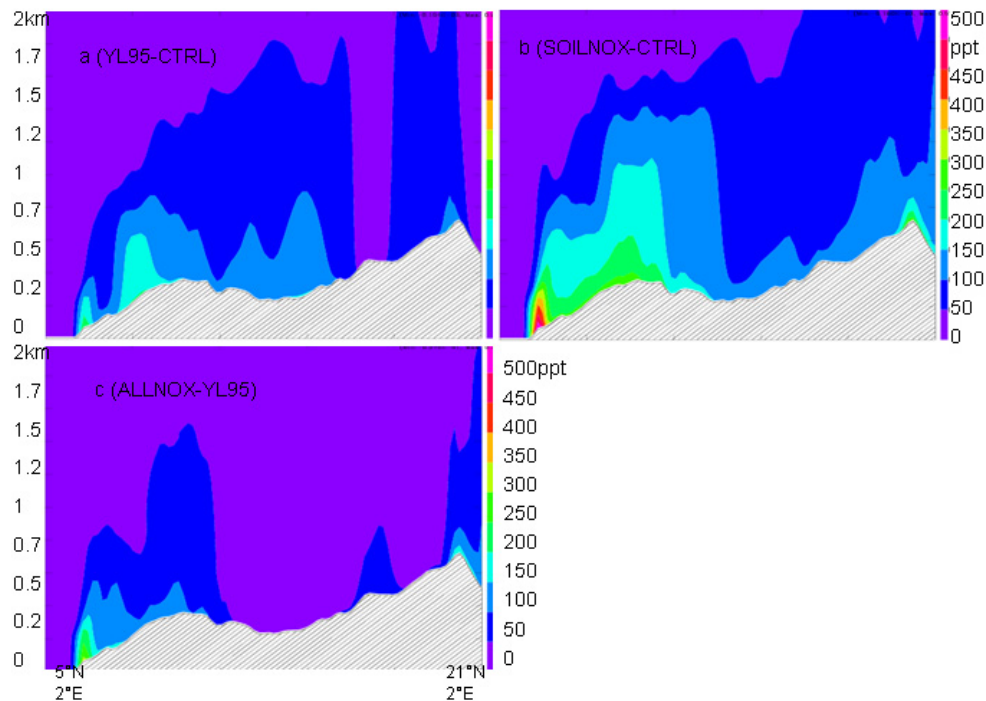
Fig. 3. Differences in NO$_x$ concentrations (ppt), from surface to 2000 m, on a North South transect at 2° E, for the 4 simulations detailed in the text: **(a)** YL95-CTRL, **(b)** SOILNOX-CTRL, **(c)** ALLNOX-YL95. 6 August 2006, 15:00 UTC.
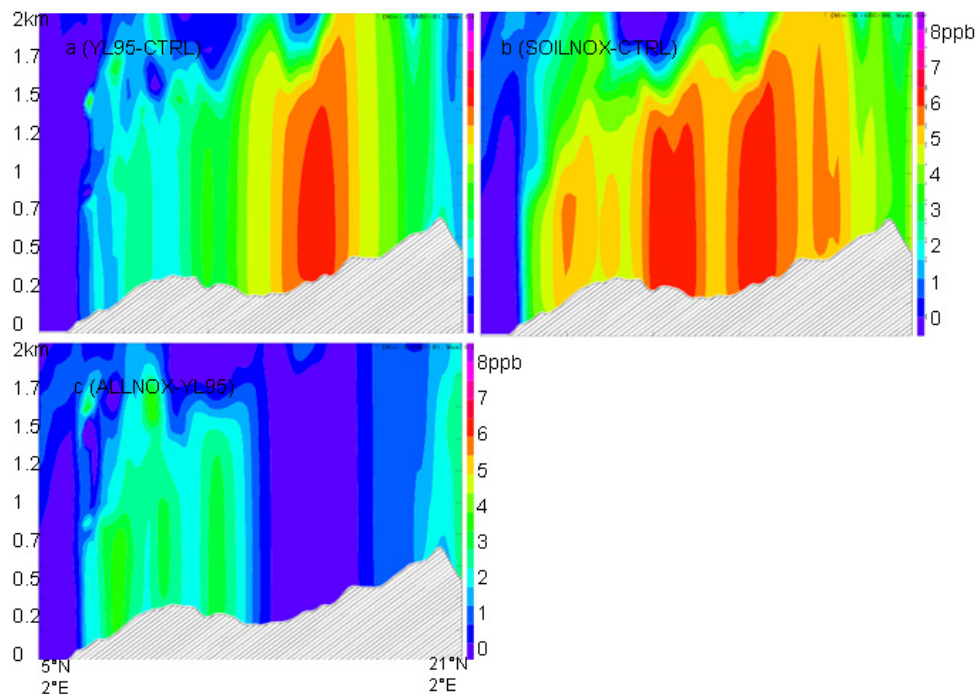
Fig. 4. Differences in O_3 concentrations (ppb), from surface to 2000 m, on a North South transect at 2° E, for the 4 simulations detailed in the text: **(a)** YL95-CTRL, **(b)** SOILNOX-CTRL, **(c)** ALLNOX-YL95, 6 August 2006, 15:00 UTC.

EGU
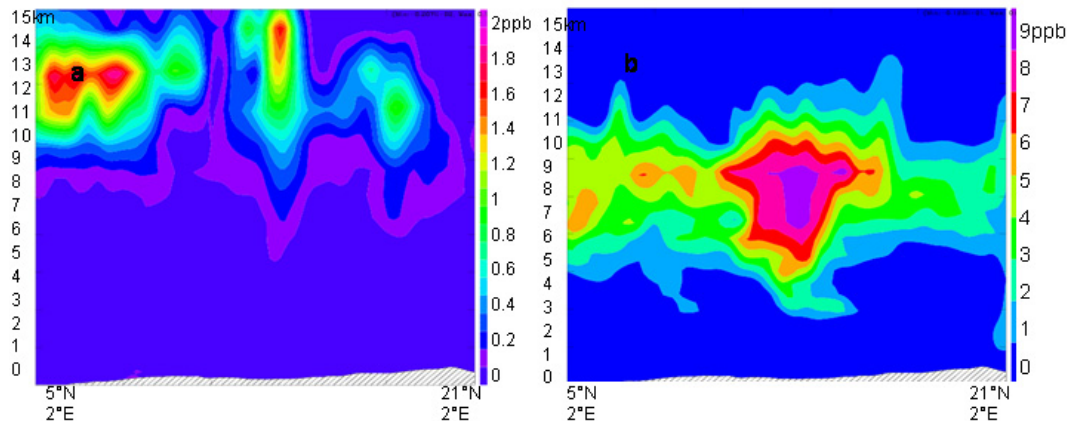
Fig. 5. Differences in **(a)** NO$_x$ concentration and **(b)** O$_3$ concentration between ALLNOX and SOILNOX simulations. 6 August 2006, 21:00 UTC.
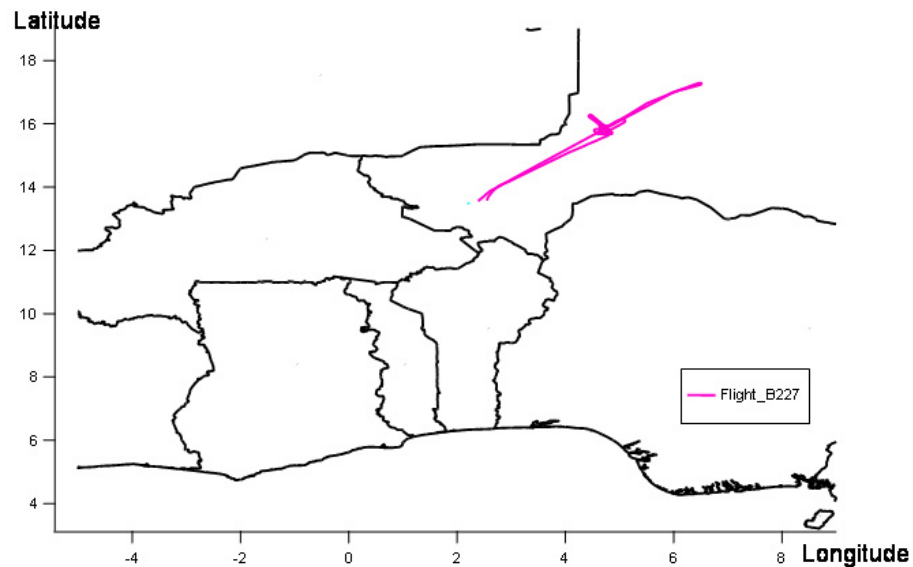
Fig. 6. The track (latitude vs. longitude) of flight B227 of the BAe-146, 6 August 2006.
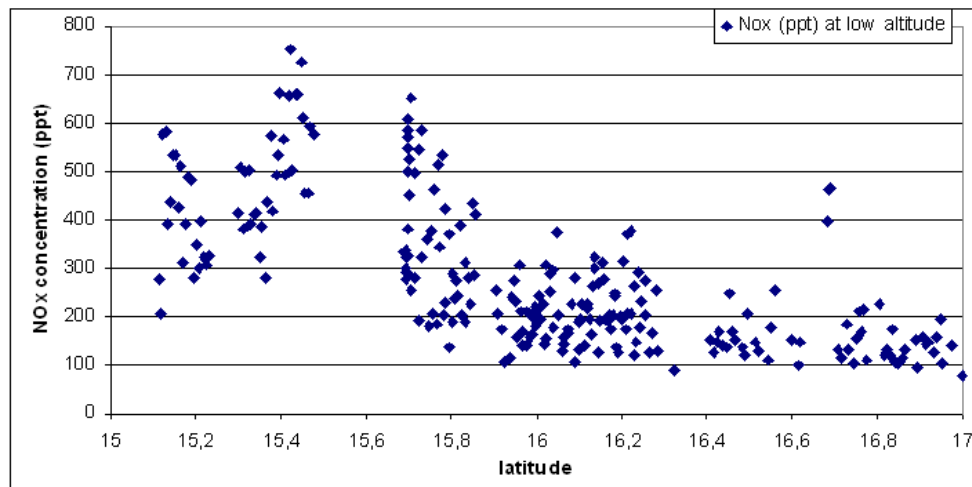
Fig. 7. NO$_x$ concentrations in ppt from the UK BAe data between 450 and 650 m, flight B227.

EGU
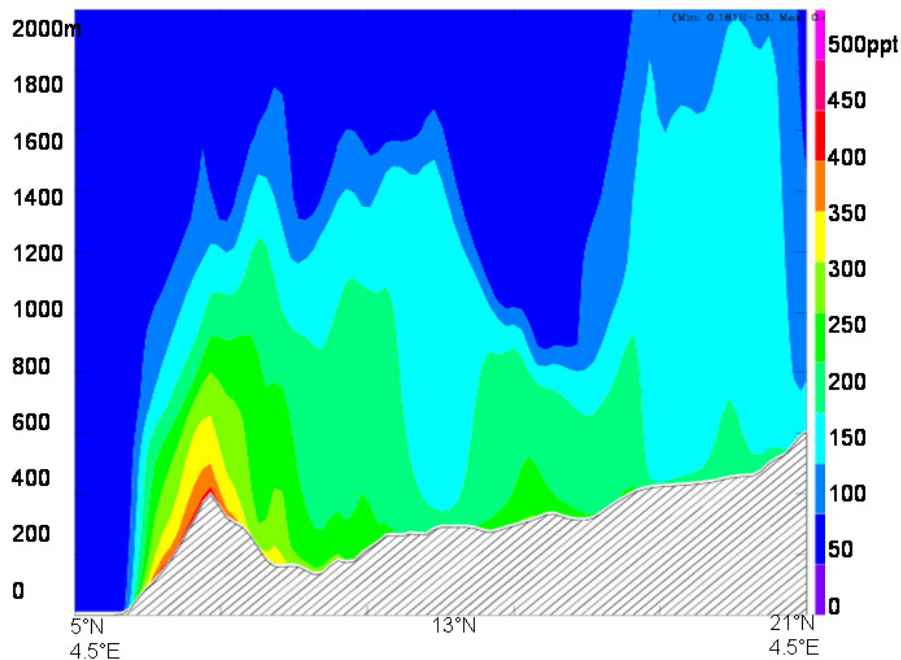
Fig. 8. Vertical cut of NO_x concentrations in ppt (4.5° E, from 5 to 21° N), ALLNOX simulation, from 0 to 2000 m. 6 August 2006, 15:00 UTC
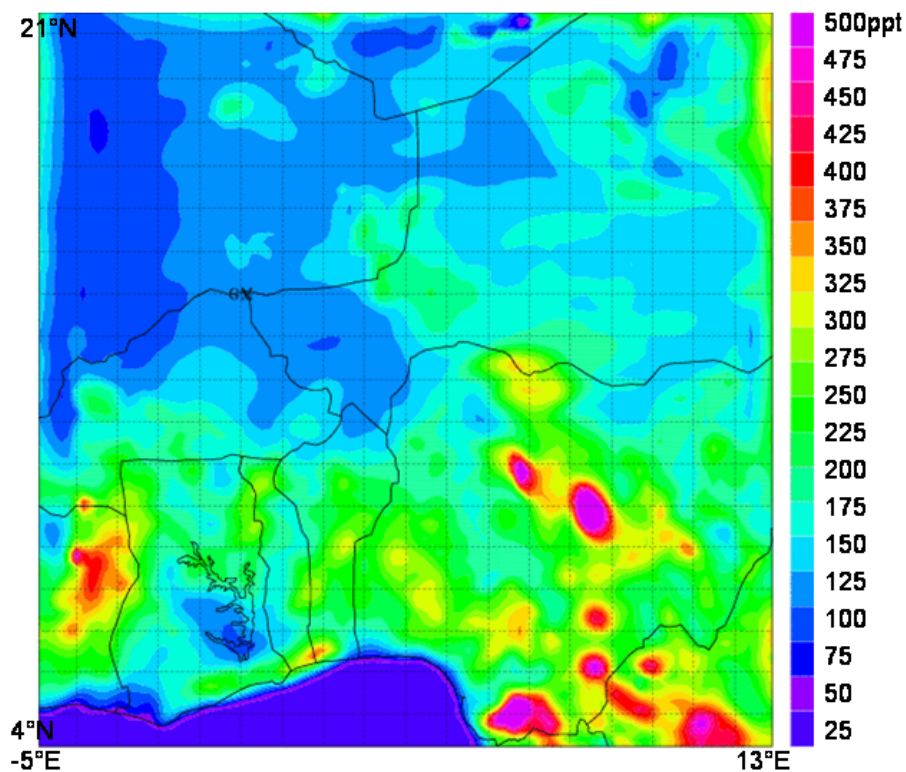
Fig. 9. NO_x concentrations in ppt, at 200-m height above ground level (corresponds to 450 m above sea level in the region of Niamey), from ALLNOX simulation at 15:00 UTC, 6 August.

EGU
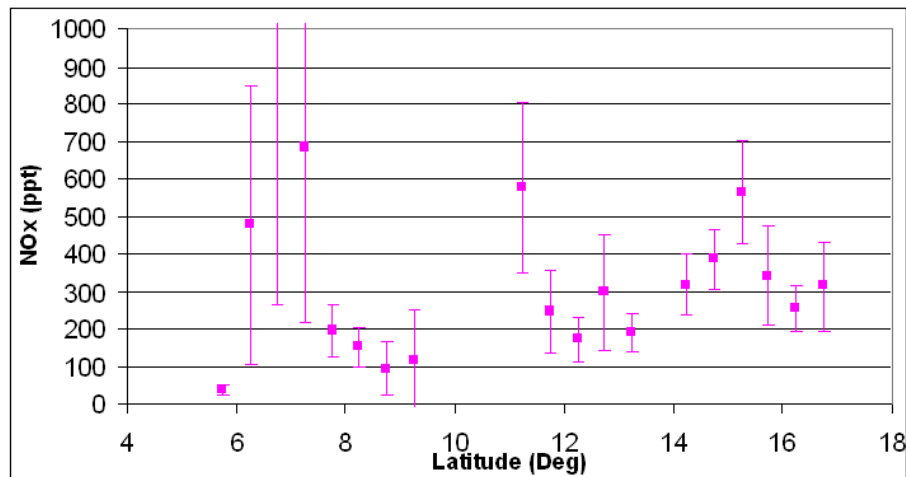
Fig. 10. NO$_x$ concentrations in ppb from the UK BAe data below 700 m, all flights.
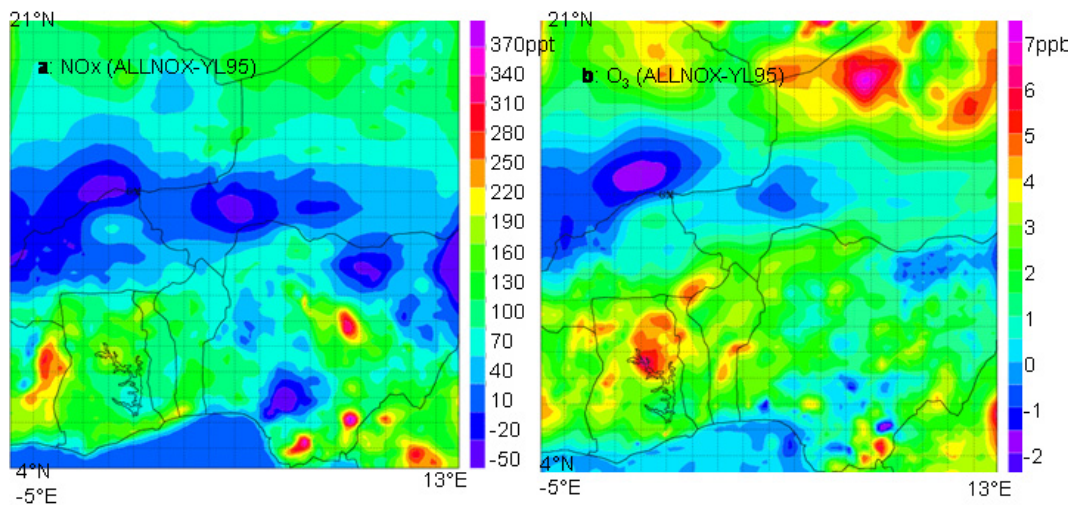
EGU

Fig. 11. Differences between ALLNOX and YL95 simulations at 200 m above ground level (corresponds to ~450 m above sea level in the region of Niamey) for **(a)** NO$_x$ concentration and **(b)** ozone concentration. 6 August 2006, 15:00 UTC.